ChemComm

Accepted Manuscript

Volume 1 | Number 1 | Jan 2013 | Pages 1–100

ChemComm

Chemical Communications
www.rsc.org/chemcomm

ROYAL SOCIETY OF CHEMISTRY

ROYAL SOCIETY OF CHEMISTRY

www.rsc.org/chemcomm

ChemComm

COMMUNICATION

A Boron Difluoride Dye with Aggregation-Induced Emission Feature and Highly Sensitive to Intra- and Extra-Cellular pH Changes

Dan Wu,[a,b] Li Shao,[a] Yang Li,[a,b] Qinglian Hu,[c] Feihe Huang,[a] Guocan Yu*[a] and Guping Tang*[b]

A novel AIE-active boron difluoride fluorescent probe P$_3$T was designed and synthesized. P$_3$T exhibited high sensitivity to intra- and extra-cellular pH changes. Furthermore, a Förster resonance energy transfer (FRET) system was
10 **constructed, where P$_3$T acted as a donor fluorophore and the DOX as the acceptor.**

In comparison to various imaging techniques, fluorescence imaging techniques show advantages in terms of excellent manoeuvrability, high spatiotemporal resolution and versatile
15 imaging agents with good biocompatibility and low radioactive risk.[1] Over the past decades, a series of new luminescent probes, including biological fluorescent proteins, metal complexes, semiconductor nanocrystals, upconversion nanophosphors and organic dyes, have been developed for bioimaging application.
20 For example, green fluorescent protein (GFP) has been widely used as a reporter of expression for morphological differentiation.[2a,2c] However, the time-consuming transfection procedures can induce unexpected morphologies and undesired abnormality in the target cells, which limits its application to
25 some extent. Currently, the commercially available quantum dots (QDs) with high luminescence and excellent photostability are the most promising fluorescent agents for long-term cell tracking.[2b,2d] Unfortunately, QDs exhibit notorious cytotoxicity due to the release of heavy metal components especially in an
30 oxidative environment, inhibiting their further bio-relevant applications. The inherent limitations of current fluorescent materials greatly hamper their physiological utilities and clinical implementation, consequently stimulating an unremitting pursuit of alternative materials with improved biochemical properties.
35 To date, efforts have been made to develop organic dyes as promising fluorescent imaging agents with lower cytotoxicity and better performance. Among various fluorophores, boradiazaindacene (BODIPY) fluorophores have gained importance in diverse applications over the past few years owing
40 to their advantageous photophysical properties,[3] including sharp absorption/emission bands, high absorption coefficients and fluorescence quantum yields. However, most of them are hydrophobic and feature planarity to some extent, which normally causes π–π stacking and other nonradiative pathways,
45 resulting in significant quenching of the emission in the aggregated state. This phenomenon is known as aggregation-

caused quenching (ACQ), which seriously limits their applications, especially in fluorescent chemosensors and bioimaging *in vitro* and *in vivo*.[4] On the other hand, the BODIPY
50 core, having a staggered N_2C_2 framework and a C_2 symmetry axis, typically exhibits a low Stokes shift (5–30 nm, in most cases), which always reduces the emission intensity due to self-absorption or the inner filter effect.

In sharp contrast to the ACQ effect, Tang and coworkers
55 developed a novel class of organic luminogens with an extraordinary aggregation-induced emission (AIE) feature, which is exactly opposite to the above-mentioned ACQ system.[5] The distinctive organic luminogens, with tetraphenylethene (TPE)[6b,6d] and hexaphenylsilole (HPS)[6a,6c] being typical examples, are non-
60 emissive in solution but are induced to luminesce intensely in the aggregate state through restriction of intramolecular rotation (RIR) of the benzene rings.[7] On account of their unique fluorescence turn-on properties with high sensitivity and contrast, a series of AIE-based fluorescent probes have emerged for living cell
65 imaging and the detection of a wide range of biomolecules over the past decade. It is urgent to fabricate new AIE-active luminogens with distinct properties that can be applied in various fields.

Herein, we designed and synthesized a novel BODIPY
70 analogue (P$_3$T) with AIE characteristics, in which one of two pyrrole units present in a BODIPY dye was replaced by quinine and the other pyrrole ring was replaced by two aromatic rings. This novel fluorophore adopted an unsymmetric propeller-shaped conformation. The resulting desymmetrization of the staggered
75 framework induced an increase of the Stokes shift caused by rendering the ground and excited states more distinct and enhanced the quantum yield effectively. More interestingly, P$_3$T was highly sensitive to intra- and extra-cellular pH changes. The emission of P$_3$T was quenched completely when it was uptaken
80 by HeLa cells due to the protonation of *N,N'*-dimethylamine group. Furthermore, an amphiphilic triblock polymer Pluronic F-127 (PF127) was utilized to encapsulated P$_3$T and doxorubicin (DOX) in the hydrophobic core of the nanoparticles (NPs) to construct a Förster resonance energy transfer (FRET) system,
85 where P$_3$T acted as a donor fluorophore and DOX as the acceptors. This ternary system as a smart drug delivery system (DDS) could simultaneously monitor the intracellular release of drug and exert therapeutic effect towards cancer cells.
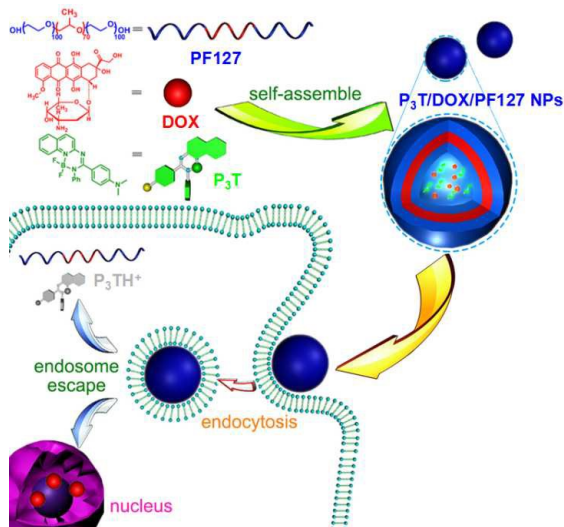
Fig. 1 Schematic illustration of the fabrication of **P₃T**/DOX/PF127 NPs and cellular uptake of **P₃T**/DOX/PF127 NPs. **P₃T**/DOX/PF127 NPs were uptaken by cells and translocated into lysosomes, the released **P₃T** was protonated and its fluorescence was quenched due to the acid
5 circumstance, while DOX was translocated to nucleus and executed its anticancer function.

P₃T was synthesized in a high yield according to the synthetic process.[8] In general, **1** and 2-bromoquinoline were added to the mixture of Pd(OAc)₂, xantphos and Cs₂CO₃ in
10 toluene, after the transition-metal catalyzed coupling reactions, the precursor product **2** was obtained. Then precursor **2** reacted readily with boron trifluoride diethyl etherate in the presence of triethylamine to yield the BF₂/amidine-based complex **P₃T** as a target molecule (Scheme 1), which is green powder. **P₃T** was
15 identified by NMR and mass spectroscopic analyses.
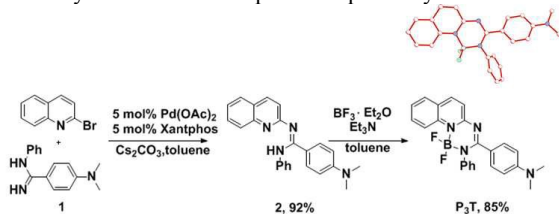
Scheme 1. Synthetic route to **P₃T** and its single-crystal structure.

First, we investigated the photophysical properties of **P₃T**. In the THF solution, **P₃T** exhibits an absorption maximum at 405
20 nm and a sharp strong green emission at 547 nm, giving a Stokes shift as large as 142 nm (Fig. 2a and 2b). When the water fraction (f_w) increased to 10%, the emission of **P₃T** was weakened effectively. On the other hand, the emission intensity remains low when the f_w value further increased to 80% (Fig. 2c). This
25 phenomenon was caused by the intramolecular charge transfer (ICT) owing to the presence of electron-donating and accepting units in **P₃T**.[9] In order to verify the ICT effect, UV/vis and fluorescence investigations were carried out in different solvent. As shown in Fig. 2a and 2b, the maximum absorption of **P₃T** in
30 the UV spectra retained at about 405 nm in different solvents with increasing polarity. The solubility and solvent polarity exerted much influence on its photoluminescence (PL) properties, with the emission maximum in hexane being 75 nm blue-shifted from that in THF. A Lippert-Mataga plot of Stokes shift against
35 the orientation polarizability of the solvent provided an upward

straight line with a small slope, confirming the ICT feature (Fig. S10).
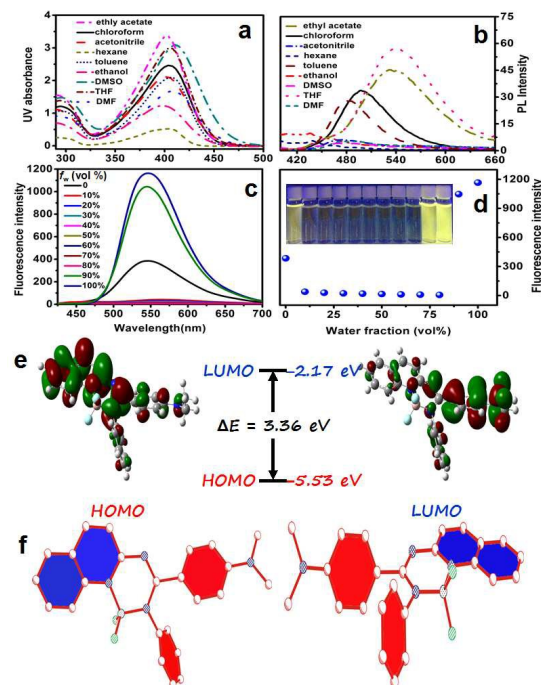
Fig. 2 (a) UV and (b) PL spectra of **P₃T** in solvents with different polarities. (c) PL spectra of **P₃T** in THF/water mixture with different f_w
40 value. (d) Plots of F/F_0 versus f_w for **P₃T** in the mixture of THF and water. Inset: fluorescent photo of the solution taken under a 365 nm UV lamp with different f_w values. (e) Molecular orbital amplitude plots of HOMO and LUMO energy levels of **P₃T**. (f) Single-crystal structures of **P₃T** from different views. Carbon atoms are white, nitrogen atoms are blue, fluorine
45 atoms are green and boron atom is grey.

Further increasing f_w value to 99%, the emission intensity increased swiftly by ~194-fold (Fig. 2d), which indicated that **P₃T** was a typical AIE-active molecule. The reason was that the solubility of **P₃T** in water was poor, aggregation of **P₃T** was
50 occurred when a large amount of water was added. The fluorescence quantum yield (Φ_F) of **P₃T** was estimated to be 34% by using fluorescein sodium as a standard (Φ_F = 0.95 in 0.1 M NaOH aqueous solution), suggesting that **P₃T** was a strong emitter in the aqueous solution. Density functional theory (DFT)
55 calculations and single-crystal structures were employed to illustrate the geometry and electronic structure of **P₃T** at the molecular level. The molecular orbital amplitude plots of the HOMO and LUMO of **P₃T** were shown in Fig. 2e. From the calculated data, HOMO and LUMO are localized on different
60 parts, HOMO is located on the donor quinoline part and LUMO is located on the acceptor part aniline part. From the calculated energy, three main allowed electronic transitions are implied, which are HOMO→LUMO (417 nm), HOMO−1→LUMO (365 nm) and the combination of HOMO−2→LUMO and
65 HOMO→LUMO+1 (364 nm). Therefore, there are two main absorption bands (~417 nm and ~365 nm) of **P₃T**. The calculated oscillator strengths (f) for the HOMO to LUMO transition and HOMO−1 to LUMO are 0.3848 and 0.3210 respectively, indicating that radioactive decay is possible. The HOMO-LUMO
70 distribution indicated that the **P₃T** probe possessed an intrinsic ICT character, in agreement with the results mentioned above.

To collect more information and to gain further insight into AIE phenomenon of **P₃T** in the aggregated state, its single-crystal structures (Fig. 2f) were grown by slow vaporation of a solution of **P₃T** in THF. **P₃T** adopts a twisted conformation due to the steric congestion between the aryl rings. The aniline ring and benzene ring twist from the planar core, similar to the propeller-shaped structure of AIE-active fluorophores. The intramolecular rotation of the aromatic rings on **P₃T** may induce the efficient nonradiative annihilation process and thus **P₃T** is nearly nonemissive in the dissolved state. However, the rotation of aniline ring and benzene ring are physically restricted effectively and the nonradiative pathways were blocked upon the addition of water, resulting in the appearance of AIE effect.
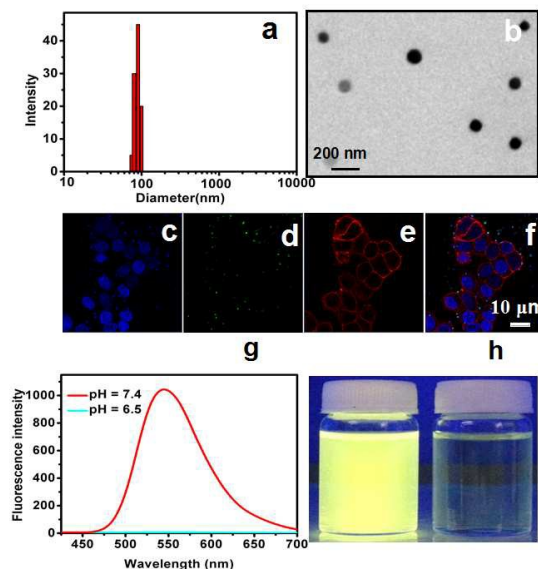
Fig. 3 (a) DLS data of the **P₃T**/PF127 NPs. (b) TEM image of **P₃T**/PF127 NPs. (c−f) Confocal microscopy images of HeLa cells upon incubation with **P₃T**/PF127 NPs (d, green) for 4 h, followed were stained with WGA (e, red) and DAPI (c, blue), and their emerge images (f). (g) PL spectra of **P₃T** at different pH values. (h) Fluorescent photos of **P₃T** solution taken under a 365 nm UV lamp at different pH values (left: pH = 7.4, right: pH = 6.5).

In order to apply this novel AIE-active fluorophore as living cell imaging agent, PF127 was utilized to encapsulate **P₃T** to prepare NPs that suitable for cellular uptake. As shown in TEM image (Fig. 3b), NPs about 100 nm in diameter were obtained by simply adding PF127 into the solution containing **P₃T** under stirring, which is suitable for cellular uptake. The average diameter of the **P₃T**-loaded NPs was measured to be 95 nm by dynamic light scattering (DLS), which was in agreement with the result obtained from TEM image (Fig. 3a). The cytotoxicity of **P₃T**/PF127 NPs towards HeLa cells was evaluated by a 3-(4′,5′-dimethylthiazol-2′-yl)-2,5-diphenyl tetrazolium bromide (MTT) assay. Fig. S12 shows that the relative cell viability is not significantly altered when the concentration of the **P₃T**/PF127 NPs increases from 25.3 to 505 μg/mL, indicating low cytotoxicity of these NPs.

Laser scanning microscopy (CLSM) was utilized to investigate the intracellular localization of the NPs. HeLa cells were labeled with blue-colored nuclei-specific DAPI and red-colored cytomembrane-specific wheat germ agglutinin conjugates (WGA), respectively. Interestingly, **P₃T** exhibited high sensitivity

to intra- and extra-cellular pH changes. The green fluorescence of the NPs mainly gathered around the cytomembrane of HeLa cells, while no fluorescence was observed in the cytoplasm. We speculated that the emission of **P₃T** was quenched completely in the cells through photoinduced electron transfer (PET) effect caused by the protonation of *N*,*N*′-dimethylamine group.[10] In order to confirm the pH-responsive property, PL spectra of **P₃T** were measured under different solution pH. As shown in Fig. 3g, **P₃T** emitted strongly at pH 7.4, while the PL intensity of **P₃T** greatly decreased when the solution pH was adjusted to 6.5, in accordance with fluorescent photos shown in Fig. 3h. To elucidate the mechanism of the fluorescence "off-on" process, the structure of the protonated state (**P₃TH⁺**) was proposed and its frontier molecular orbital (FMO) energies were calculated using Gaussian 09 (DFT/TDDFT in B3LYP/6-31+G(d) level), which were shown in Table S1. In **P₃TH⁺** state, there is PET between quinoline part and aniline part. The oscillator strengths are all notably lower for the transitions after the protonation, especially the transition of HOMO−1→LUMO ($f = 0.0129$) is now nearly forbidden in **P₃TH⁺**. Besides, the gaps between LUMO, LUMO+1 and LUMO+2 are much smaller in **P₃TH⁺**, which would also much facilitate the internal conversion in **P₃TH⁺**. As a result, **P₃TH⁺** could not complete a fluorescence process as facilely as **P₃T**. On the other hand, quenched **P₃TH⁺** could turn back to luminescent **P₃T**, which was confirmed by ¹HNMR spectrum (Fig. S8 and S9).
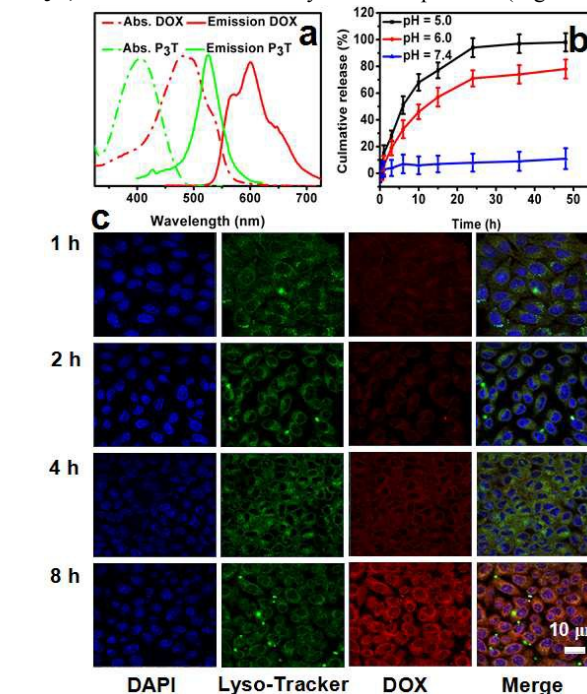
Fig. 4 (a) UV and PL spectra of **P₃T** and DOX. (b) Release profiles of the DOX from the **P₃T**/DOX/PF127 NPs under different solution pH. (c) Confocal microscopy images of HeLa cells upon incubation with **P₃T**/DOX/PF127 NPs for 1, 2, 4, and 8 h respectively, then were stained with DAPI (blue) and Lyso-Tracker (green).

FRET is a well-established energy transfer process between two fluorophores that is very sensitive to changes at the nanometer-scale in the donor-to-acceptor separation distance,[11] which has been extensively employed to construct protein-, nucleic acid-based and mimetic nanoprodrug bioprobes.[12] In our studies, we found that there is a spectral overlap between the

emission spectrum of **P₃T** and the absorption spectrum of DOX (Fig. 4a). A FRET system was fabricated by encapsulating **P₃T** and DOX in the hydrophobic core of PF127 NPs, where **P₃T** acted as a donor fluorophore and the DOX as the acceptors. As shown in Fig. S11, the PL intensity of **P₃T** decreased gradually and the PL intensity of DOX increased slightly upon addition of DOX, which confirmed the energy transfer from **P₃T** to DOX.[11b]

The release kinetics of DOX at different pH was investigated shown in Fig. 4b. Negligible release of DOX was observed over a period of 24 h under physiological conditions (pH 7.4), indicating that most DOX still stayed in the core of the ternary NPs. When the solution pH was decreased to 6.0, the release of DOX from **P₃T**/DOX/PF127 NPs became quick and about 70% of DOX was released during the same period. The release rate of the encapsulated drug molecules became much faster and nearly 100% of DOX was released at lysosome environment (pH 5.0). The microscopic occurrence of drug release was also monitored by CLSM. HeLa cells were incubated with **P₃T**/DOX/PF127 NPs for 1 h, 2 h, 4 h, and 8 h, respectively. As shown in Fig. 4c, weak red fluorescence was well overlapped with the green fluorescence arising from Lyso-Tracker after 1h incubation, demonstrating that the DOX in the core of **P₃T**/DOX/PF127 NPs was released in the lysosomes due to the relatively low pH environment. With time elapsing, the red fluorescence became stronger, indicating that DOX was released gradually after internalizing by the cells, Especially for the cells cultured with **P₃T**/DOX/PF127 NPs for 8h, red fluorescence was observed in the nucleus, which emphasized that DOX released from **P₃T**/DOX/PF127 NPs was escaped from lysosomes and translocated to nucleus. On the basis of these *in vitro* experiments, we confirmed that this ternary system could be used as a smart DDS. The cytotoxicity of **P₃T**/DOX/PF127 NPs and free DOX towards HeLa cells was evaluated by MTT assay. It was found that relative cell viability of **P₃T**/DOX/PF127 NPs against cancer cells after 24 h showed similar therapeutic effects as the free DOX (Fig. S13), indicating that **P₃T**/DOX/PF127 NPs remained therapeutic effect towards cancer cells.

In summary, an unsymmetric N_3C_2/BF_2 organic fluorophore **P₃T** was designed and successfully synthesized. **P₃T** exhibited an ICT effect caused by the donor-acceptor interaction between the quinoline group and the aniline unit. Whereas it emitted faintly in solution, it became highly emissive in the aggregated state, demonstrating an attracting phenomenon of aggregation-induced emission. It was highly sensitive to intra- and extra-cellular pH changes. The emission of **P₃T** was quenched completely after it was uptaken by HeLa cells due to the protonation of *N,N'*-dimethylamine group. On the other hand, **P₃T** and DOX were encapsulated into the hydrophobic core of PF127 to construct a FRET system, where **P₃T** acted as the donor and DOX as the acceptor. This ternary system also turned out to be a smart drug delivery system. It not only could realize controlled drug release, but also remain its therapeutic effect of DOX towards the cancerous HeLa cells. Absolutely, this novel AIEgen with high sensitivity to intra- and extra-cellular pH changes will not only enrich the family of AIEgens and find wide application in chemosensors and bioprobes etc., but also attract considerable attentions from scientists in the areas of fundamental photophysical research and material sciences.

Notes and references

a Department of Chemistry, Zhejiang University, 310028 Hangzhou, P. R. China. E-mail: guocanyu@zju.edu.cn
b Institute of Chemical Biology and Pharmaceutical Chemistry, Department of Chemistry, Zhejiang University, 310027 Hangzhou, P. R. China. E-mail: tangguping@zju.edu.cn
c College of Biological and Environmental Engineering, Zhejiang University of Technology, 310014 Hangzhou, P. R. China.
† Electronic Supplementary Information (ESI) available: [Experiamental details, Lipper plot, DFT calculation of **P₃TH⁺**, ^{1}H NMR, 2D COSY spectra, ESI mass spectra and X-ray crystal data of **P₃T**]. See DOI: 10.1039/b000000x/

1   (a) D. W. Domaille, E. L. Que and C. J. Chang, *Nat. Chem. Biol.* 2008, **4**, 168; (b) H. Kobayashi, M. Ogawa, R. Alford, P. L. Choyke and Y. Urano, *Chem. Rev.*, 2010, **110**, 2620; (c) T. Ueno and T. Nagano, *Nat. Methods.*, 2011, **8**, 642.

2   (a) N. C. Shaner, R. E. Campbell, P. A. Steinbach, B. N. Giepmans, A. E. Palmer and R. Y. Tsien, *Nat. Biotechnol.*, 2004, **22**, 1567; (b) A. M. Derfus, W. C. W. Chan and S. N. Bhatia, *Nano Lett.*, 2004, **4**, 11; (c) K. P. Kent, W. Childs and S. G. Boxer, *J. Am. Chem. Soc.*, 2008, **130**, 9664; (d) S. J. Rosentha, J. C. Chang, O. Kovtun, J. R. McBride and I. D. Tomlinson, *Chem. Biol.*, 2011, **18**, 10; (e) T. T. Chen, Y. H. Hu, Y. Cen, X. Chu and Y. Lu, *J. Am. Chem. Soc.*, 2013, **31**, 11595.

3   (a) W. L. Zhao and E. M. Carreira, *Chem. Eur. J.*, 2006, **12**, 7254; (b) A. Loudet and K. Burgess, *Chem. Rev.*, 2007, **107**, 4891; (c) G. Ulrich, R. Ziessel and A. Harriman, *Angew. Chem. Int. Ed.*, 2008, **47**, 1184; (d) M. E. El-Khouly, A. N. Amin, M. E. Zandler, S. Fukuzumi and F. D'Souza, *Chem. Eur. J.*, 2012, **18**, 5239.

4   (a) A. C. Grimsdale, K. Leok Chan, R. E. Martin, P. G. Jokisz and A. B. Holmes, *Chem. Rev.*, 2009, **109**, 897; (b) J. Z. Liu, J. W. Y. Lam and B. Z. Tang, *Chem. Rev.*, 2009, **11**, 5799.

5   (a) Y. N. Hong, J. W. Y. Lam, and B. Z. Tang, *Chem. Commun.*, 2009, 4332; (b) Y. N. Hong, J. W. Y. Lam and B. Z. Tang, *Chem. Soc. Rev.*, 2011, **40**, 5361.

6   (a) L. P. Heng, Y. Q. Dong, J. Zhai, B. Z. Tang and L. Jiang, *Langmuir.*, 2008, **24**, 2157; (b) Y. Liu, C. M. Deng, L. Tang, A. J. Qin, R. G. Hu, J. Z. Sun and B. Z Tang, *J. Am. Chem. Soc.*, 2011, **4**, 660; (c) G. Yu, S. W. Yin, Y. Q. Liu, J. S. Chen, X. J. Xu, X. B. Sun, D. G. Ma, X. W. Zhan, Q. Peng, Z. G. Shuai, B. Z. Tang, D. B. Zhu, W. H. Fang, Y. Luo, *J. Am. Chem. Soc.*, 2013, **127**, 6335; (d) X. D. Lou, Z. J. Zhao, Y. N. Hong, C. Dong, X. H. Min, Y. Zhuang, X. M. Xu, Y. M. Jia, F. Xia and Y. M. Tang, *Nanoscale*, 2014, **6**, 14691.

7   (a) J. Q. Shi, N. Chang, C. H. Li, J. Mei, C. M. Deng, X. L. Luo, Z. P. Liu, Z. S. Bo, Y. Q. Dong and B. Z. Tang, *Chem. Commun.*, 2012, **86**, 10675; (b) C. Fang, Y. J. Xie, M. R. Johnston, Y. L. Ruan, B. Z. Tang, Q. Peng and Y. H. Tang, *J. Phys. Chem. A*, 2015, **29**, 8049.

8   D. B. Zhao, G. C. Li, D. Wu, X. R. Qin, P. Neuhaus, Y. Y. Cheng, S. J. Yang, Z. Y. Lu, X. M. Pu, C. Long and J. S. You, *Angew. Chem. Int. Ed.*, 2013, **52**, 13676 .

9   (a) S. Cogan, S. Zilberg and Y. Haas, *J. Am. Chem. Soc.*, 2006, **128**, 3335; (b) J. S. Yang, K. L. Liau, C. Y. Li and M. Y. Chen, *J. Am. Chem. Soc.*, 2007, **129**, 13183; (c) H. Chen, W. Y. Lin, W. Q. Jiang, B. L. Dong, H. J. Cui and Y. H. Tang, *Chem. Commun.*, 2015, **32**, 6968.

10 (a) H. Zhang, J. L. Fan, J. Y. Wang, S. Z. Zhang, B. R. Dou and X. J. Peng, *J. Am. Chem. Soc.*, 2013, **135**, 11663; (b) B. Daly, J. Ling and A. Prasanna de Silva, *Chem. Soc. Rev.*, 2015, **44**, 4203.

11 (a) J. P. Lai, B. P. Shah, E. Garfunkel and K. B. Lee, *ACS Nano*, 2013, **3**, 2741; (b) L. Yuan, W. Y. Lin, K. B. Zheng and S. S. Zhu, *Acc. Chem. Res.*, 2013, **7**, 1462.

12 (a) C. Y. Zhang, H. C. Yeh, M. T. Kuroki and T. H. Wang, *Nat. Mater.*, 2005, **4**, 826; (b) D. D. Su, C. L. Teoh, S. Sahu, R. K. Das, Y. Yang, *Biomaterials*, 2014, **35**, 6078.

Colour Graphic：
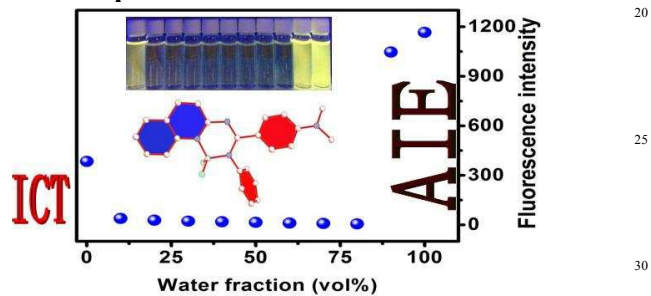
Text:

A novel AIE-active boron difluoride fluorescent probe **P₃T** was designed and synthesized. **P₃T** exhibited high sensitivity to intra- and extra-cellular pH changes. Furthermore, a Förster resonance energy transfer (FRET) system was constructed, where **P₃T** acted as a donor fluorophore and the DOX as the acceptor.